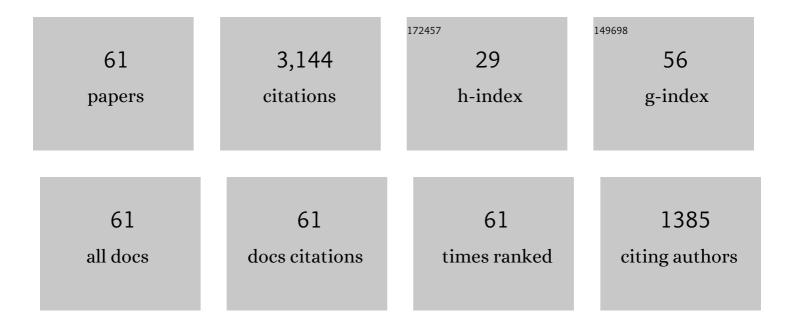
List of Publications by Year in descending order

Source: https://exaly.com/author-pdf/8500785/publications.pdf Version: 2024-02-01



#	Article	IF	CITATIONS
1	Effects of the vertical plasma drift velocity on the generation and evolution of equatorial spreadF. Journal of Geophysical Research, 1999, 104, 19859-19869.	3.3	590
2	GPS and ionospheric scintillations. Space Weather, 2007, 5, .	3.7	492
3	Gravity wave initiation of equatorial spread F/plasma bubble irregularities based on observational data from the SpreadFEx campaign. Annales Geophysicae, 2009, 27, 2607-2622.	1.6	183
4	Fading timescales associated with GPS signals and potential consequences. Radio Science, 2001, 36, 731-743.	1.6	118
5	Size, shape, orientation, speed, and duration of GPS equatorial anomaly scintillations. Radio Science, 2004, 39, n/a-n/a.	1.6	103
6	Conjugate Point Equatorial Experiment (COPEX) campaign in Brazil: Electrodynamics highlights on spread <i>F</i> development conditions and dayâ€toâ€day variability. Journal of Geophysical Research, 2009, 114, .	3.3	90
7	Global Positioning System measurements of the ionospheric zonal apparent velocity at Cachoeira Paulista in Brazil. Journal of Geophysical Research, 2000, 105, 5317-5327.	3.3	75
8	Abnormal evening vertical plasma drift and effects on ESF and EIA over Brazilâ€ S outh Atlantic sector during the 30 October 2003 superstorm. Journal of Geophysical Research, 2008, 113, .	3.3	72
9	The São LuÃs 30 MHz coherent scatter ionospheric radar: System description and initial results. Radio Science, 2004, 39, n/a-n/a.	1.6	69
10	Equatorial ionospheric vertical plasma drift model over the Brazilian region. Journal of Geophysical Research, 1996, 101, 10887-10892.	3.3	65
11	Observed solar radio burst effects on GPS/Wide Area Augmentation System carrier-to-noise ratio. Space Weather, 2006, 4, n/a-n/a.	3.7	64
12	lonospheric zonal velocities at conjugate points over Brazil during the COPEX campaign: Experimental observations and theoretical validations. Journal of Geophysical Research, 2009, 114, .	3.3	59
13	Latitudinal variations of scintillation activity and zonal plasma drifts in South America. Radio Science, 2002, 37, 6-1-6-7.	1.6	58
14	The variability of low″atitude ionospheric amplitude and phase scintillation detected by a tripleâ€frequency GPS receiver. Radio Science, 2017, 52, 439-460.	1.6	57
15	GPS availability and positioning issues when the signal paths are aligned with ionospheric plasma bubbles. GPS Solutions, 2018, 22, 1.	4.3	49
16	Overview and summary of the Spread F Experiment (SpreadFEx). Annales Geophysicae, 2009, 27, 2141-2155.	1.6	48
17	Equatorial spreadFirregularity characteristics over São LuÃs, Brazil, using VHF radar and GPS scintillation techniques. Radio Science, 2004, 39, n/a-n/a.	1.6	47
18	Scintillationâ€producing Fresnelâ€scale irregularities associated with the regions of steepest TEC gradients adjacent to the equatorial ionization anomaly. Journal of Geophysical Research, 2010, 115, .	3.3	47

#	Article	IF	CITATIONS
19	Modelling of the total electronic content and magnetic field anomalies generated by the 2011 Tohoku-Oki tsunami and associated acoustic-gravity waves. Geophysical Journal International, 2012, , no-no.	2.4	46
20	Analysis of the Characteristics of Low-Latitude GPS Amplitude Scintillation Measured During Solar Maximum Conditions and Implications for Receiver Performance. Surveys in Geophysics, 2012, 33, 1107-1131.	4.6	45
21	The impact of gravity waves rising from convection in the lower atmosphere on the generation and nonlinear evolution of equatorial bubble. Annales Geophysicae, 2009, 27, 1657-1668.	1.6	40
22	Climatology and modeling of ionospheric scintillations and irregularity zonal drifts at the equatorial anomaly crest region. Annales Geophysicae, 2017, 35, 1201-1218.	1.6	40
23	Understanding spaced-receiver zonal velocity estimation. Journal of Geophysical Research, 2004, 109, .	3.3	39
24	On the distribution of GPS signal amplitudes during low-latitude ionospheric scintillation. GPS Solutions, 2013, 17, 499-510.	4.3	37
25	Extended ionospheric amplitude scintillation model for GPS receivers. Radio Science, 2014, 49, 315-329.	1.6	37
26	Mapping and Survey of Plasma Bubbles over Brazilian Territory. Journal of Navigation, 2007, 60, 69-81.	1.7	36
27	Survey and prediction of the ionospheric scintillation using data mining techniques. Space Weather, 2010, 8, n/a-n/a.	3.7	35
28	Ionospheric irregularity behavior during the September 6–10, 2017 magnetic storm over Brazilian equatorial–low latitudes. Earth, Planets and Space, 2019, 71, .	2.5	34
29	Effects of the fringe field of Rayleigh-Taylor instability in the equatorialEand valley regions. Journal of Geophysical Research, 2004, 109, .	3.3	32
30	Multi-technique investigations of storm-time ionospheric irregularities over the São LuÃs equatorial station in Brazil. Annales Geophysicae, 2004, 22, 3513-3522.	1.6	30
31	Climatology of the scintillation onset over southern Brazil. Annales Geophysicae, 2018, 36, 565-576.	1.6	30
32	Coherent backscatter radar imaging in Brazil: large-scale waves in the bottomside F-region at the onset of equatorial spread <i>F</i> . Annales Geophysicae, 2008, 26, 3355-3364.	1.6	29
33	Statistical evaluation of GLONASS amplitude scintillation over low latitudes in the Brazilian territory. Advances in Space Research, 2018, 61, 1776-1789.	2.6	28
34	A Three-Dimensional Simulation of Collisional-Interchange-Instability in the Equatorial-Low-Latitude Ionosphere. Space Science Reviews, 2005, 121, 253-269.	8.1	25
35	Magnetic conjugate point observations of kilometer and hundredâ€meter scale irregularities and zonal drifts. Journal of Geophysical Research, 2010, 115, .	3.3	25
36	Investigating Ionospheric Scintillation Effects on Multifrequency GPS Signals. Surveys in Geophysics, 2021, 42, 999-1025.	4.6	25

#	Article	IF	CITATIONS
37	Equatorial scintillation calculations based on coherent scatter radar and C/NOFS data. Radio Science, 2011, 46, .	1.6	23
38	Storm-time total electron content and its response to penetration electric fields over South America. Annales Geophysicae, 2011, 29, 1765-1778.	1.6	23
39	Ionospheric Scintillation and Dynamics of Fresnel-Scale Irregularities in the Inner Region of the Equatorial Ionization Anomaly. Surveys in Geophysics, 2013, 34, 233-251.	4.6	21
40	C/NOFS and radar observations during a convective ionospheric storm event over South America. Geophysical Research Letters, 2009, 36, .	4.0	18
41	Tomographic imaging of the equatorial and low-latitude ionosphere over central-eastern Brazil. Earth, Planets and Space, 2011, 63, 129-138.	2.5	16
42	On the characteristics of 150-km echoes observed in the Brazilian longitude sector by the 30 MHz São LuÃs radar. Annales Geophysicae, 2011, 29, 1905-1916.	1.6	16
43	Thermospheric Meridional Wind Control on Equatorial Scintillations and the Role of the Evening F-Region Height Rise, EÂ×ÂB Drift Velocities and F2-Peak Density Gradients. Surveys in Geophysics, 2010, 31, 509-530.	4.6	15
44	Performance of 6 Different Global Navigation Satellite System Receivers at Low Latitude Under Moderate and Strong Scintillation. Earth and Space Science, 2021, 8, e2020EA001314.	2.6	14
45	The GNSS NavAer INCT Project Overview and Main Results. Journal of Aerospace Technology and Management, 0, 14, .	0.3	14
46	VHF radar observations of the dip equatorial E-region during sunset in the Brazilian sector. Annales Geophysicae, 2006, 24, 1617-1623.	1.6	13
47	Equatorial 150 km echoes and daytime F region vertical plasma drifts in the Brazilian longitude sector. Annales Geophysicae, 2013, 31, 1867-1876.	1.6	11
48	The Acoustic Gravity Wave Induced Disturbances in the Equatorial Ionosphere. , 2011, , 141-162.		9
49	Modulation of equatorial electrojet plasma waves by overshielding electric field during geomagnetic storms. Journal of Geophysical Research, 2011, 116, n/a-n/a.	3.3	8
50	lmaging equatorial spread <i>F</i> irregularities with the São LuÃs coherent backscatter radar interferometer. Radio Science, 2012, 47, .	1.6	7
51	Atmospheric Gravity Waves Observed in the Nightglow Following the 21 August 2017 Total Solar Eclipse. Geophysical Research Letters, 2020, 47, e2020GL088924.	4.0	7
52	Equatorial zonal electric fields inferred from a 3â€D electrostatic potential model and groundâ€based magnetic field measurements. Journal of Geophysical Research, 2009, 114, .	3.3	6
53	Ionospheric Disturbances Observed Following the Ridgecrest Earthquake of 4 July 2019 in California, USA. Remote Sensing, 2022, 14, 188.	4.0	6
54	Performance analysis of <i>κ</i> - <i>μ</i> distribution for Global Positioning System (GPS) L1 frequency-related ionospheric fading channels. Journal of Space Weather and Space Climate, 2019, 9, A15.	3.3	5

#	Article	IF	CITATIONS
55	An amplitude scintillation test pattern standard for evaluating GPS receiver performance. Space Weather, 2005, 3, n/a-n/a.	3.7	4
56	Lâ€Band Synthetic Aperture Radar Observation of Ionospheric Density Irregularities at Equatorial Plasma Depletion Region. Geophysical Research Letters, 2021, 48, e2021GL093541.	4.0	3
57	Conjugated asymmetry of the onset and magnitude of GPS scintillation driven by the vertical plasma drift. GPS Solutions, 2022, 26, 1.	4.3	3
58	A GPS signal-in-space simulation model for equatorial and low latitudes in the Brazilian longitude sector. GPS Solutions, 2022, 26, .	4.3	2
59	Longitudinal ionospheric effects in the South Atlantic evening sector during solar maximum. Journal of Geophysical Research, 2002, 107, SIA 3-1.	3.3	1
60	Numerical Modeling of Coseismic Tropospheric Disturbances Arising from the Unstable Acoustic Gravity Wave Energetics. Atmosphere, 2021, 12, 765.	2.3	0
61	Mesosphere–lonosphere Coupling Processes Observed in the F Layer Bottom-Side Oscillation. , 2011, , 163-175.		0